

## PUSHING THE LIMITS: K2 OBSERVATIONS OF THE TRANS-NEPTUNIAN OBJECTS 2002 GV<sub>31</sub> AND (278361) 2007 JJ<sub>43</sub>

A. PÁL<sup>1,2</sup>, R. SZABÓ<sup>1</sup>, GY. M. SZABÓ<sup>1,3,4</sup>, L. L. KISS<sup>1,4,5</sup>, L. MOLNÁR<sup>1</sup>, K. SÁRNECZKY<sup>1,4</sup>, AND CS. KISS<sup>1</sup>

*Draft version October 15, 2018*

### ABSTRACT

We present the first photometric observations of trans-Neptunian objects (TNOs) taken with the *Kepler* space telescope, obtained in the course of the K2 ecliptic survey. Two faint objects have been monitored in specifically designed pixel masks that were centered on the stationary points of the objects, when their daily motion was the slowest. In the design of the experiment, only the apparent path of these objects were retrieved from the detectors, i.e. the costs in terms of Kepler pixels were minimized. Because of the faintness of the targets we employ specific reduction techniques and co-added images. We measure rotational periods and amplitudes in the unfiltered *Kepler* band as follows: for (278361) 2007 JJ<sub>43</sub> and 2002 GV<sub>31</sub> we get  $P_{rot} = 12.097$  h and  $P_{rot} = 29.2$  h while 0.10 and 0.35 mag for the total amplitudes, respectively. Future space missions, like TESS and PLATO are not well suited to this kind of observations. Therefore, we encourage to include the brightest TNOs around their stationary points in each observing campaign to exploit this unique capability of the K2 Mission – and therefore to provide unbiased rotational, shape and albedo characteristics of many objects.

*Subject headings:* methods: observational — techniques: photometric — astrometry — minor planets, asteroids: general — Kuiper belt objects: individual (2002 GV<sub>31</sub>, (278361) 2007 JJ<sub>43</sub>)

### 1. INTRODUCTION

*Kepler* has provided incredible results on extrasolar planets and planetary systems, as well as on stellar astrophysics. After analyzing main-belt asteroids (Szabó et al. 2015), here we continue the exploration of our own Solar System by pushing the limits of the spacecraft and observing faint, trans-Neptunian objects.

The *Kepler* spacecraft is equipped with a 0.95-m Schmidt telescope and 42 imaging CCDs, from which 38 are currently in operation. *Kepler* was designed to be the most precise photometer in order to detect the transits of numerous small planets (Borucki et al. 2010). It monitored approximately 170 000 targets in the Lyra-Cygnus field, at high Ecliptic latitudes, almost continuously for four years during its primary mission. But after the failure of two reaction wheels the telescope permanently lost its ability to maintain that attitude. Soon a new mission, called K2, was initiated to save the otherwise healthy and capable space telescope (Howell et al. 2014). Since then, *Kepler* has been observing in shorter, 75-day-long campaigns along the Ecliptic to balance the radiation pressure from the Sun.

The ecliptic fields include innumerable Solar System objects, although most asteroids and planets cross the field-of-view quite quickly. TNOs, in contrast, appear

to move slowly around their stationary points, and can be observed for extended periods of time. The 4''/pixel resolution of the CCDs is sufficient to avoid confusion even for faint targets. But the observations posed various challenges for *Kepler*. Even the brighter TNOs are at the detection limit of the telescope ( $V = 20 - 22$  mag), with an expected precision of a few tenths of a magnitude for a single long-cadence (30-min) observation. Moreover, TNOs exhibit quadratically increasing proper motions away from the stationary points. Since the pixel mask allocation is fixed for an entire campaign, the whole length of the orbital arc has to be observed continuously. Despite these challenges, the K2 mission is in a unique position to gather continuous TNO light curves in white light.

The rotational light curve of small bodies in the Solar System is determined by the shape and albedo variations on the surface of the target, and provides information on these important characteristics. In addition, the collisional history of these bodies is stored in the spin state of the objects, probing different eras of the Solar Systems's debris disk evolution depending on the size. The largest objects ( $\sim 500$  km or larger in diameter) decoupled early from collisional evolution of the debris disks, therefore their rotation should reflect the cumulative effect of collisions during the formation period. Medium size objects (100 – 500 km) likely avoided catastrophic impacts with a rotation affected by smaller past events, while the smallest bodies ( $< 100$  km) are probably remnants of several collisions during the evolution of the Solar System's debris disc (for more details, see also Lacerda 2005).

In order to study the rotational properties of TNOs we proposed a pilot study for K2 Campaign 1 to observe the object 2002 GV<sub>31</sub> ( $V \approx 22.5$  mag) with a small pixel mask for a limited time around the stationary point (pro-

Electronic address: apal@szofi.net

<sup>1</sup> Konkoly Observatory, Research Centre for Astronomy and Earth Sciences, Hungarian Academy of Sciences, H-1121 Budapest, Konkoly Thege Miklós út 15-17, Hungary

<sup>2</sup> Eötvös Loránd Tudományegyetem, H-1117 Pázmány Péter sétány 1/A, Budapest, Hungary

<sup>3</sup> ELTE Gothard Astrophysical Observatory, H-9704 Szombathely, Szent Imre herceg út 112, Hungary

<sup>4</sup> Gothard-Lendület Research Team, H-9704 Szombathely, Szent Imre herceg út 112, Hungary

<sup>5</sup> Sydney Institute for Astronomy, School of Physics A28, University of Sydney, NSW 2006, Australia

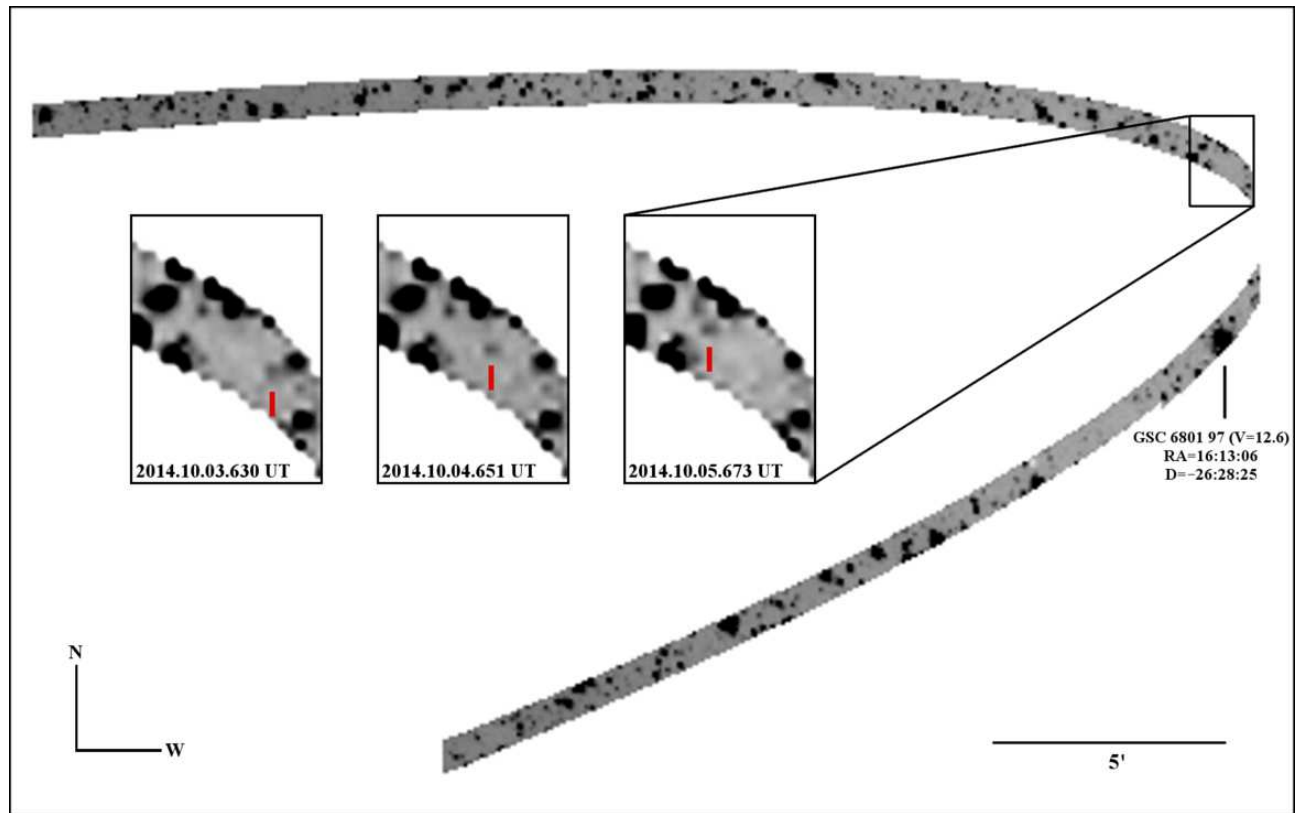


FIG. 1.— Trajectory of (278361) 2007 JJ<sub>43</sub> and the allocated 661  $1 \times 11$  and  $1 \times 13$  pixel stripes on the CCD module #17 of the *Kepler* space telescope. In the insets we show three individual exposures along the arc after the stationary point which unfortunately fell off silicon. The small inserts show an area of  $1.3' \times 1.8'$ .

posid: GO1064). The field of Campaign 2 included multiple moderately bright targets from which ultimately only (278361) 2007 JJ<sub>43</sub> ( $V \approx 20.25$  mag) was selected for observation (Proposal IDs GO2066 and GO3053).

## 2. OBSERVATIONS

For 2002 GV<sub>31</sub> a rectangular,  $23 \times 22$ -pixel mask was allocated by the Guest Observer Office that included the object for 16 days around its stationary point, but 2.8 days were lost to a mid-campaign data download period. In contrast, 2007 JJ<sub>43</sub> was covered with a long arc constructed from a mosaic of 661 small ( $1 \times 11$  or  $1 \times 13$ ) pixel masks, but the region of the stationary point itself fell off silicon. This caused a 20.9 d long gap in the observations, separating the data into a 18.7 d and a 39.2 d long section.

The elongation of the object decreased from 135 to 60 degrees during the campaign. The public target pixel time series files from the C1 and C2 fields were retrieved from the MAST archive<sup>6</sup> for the respective observations.

Without stabilization around the third axis, the *Kepler* space telescope slowly rolls about the optical axis. This movement causes the field-of-view to rotate slightly and it is corrected by the on-board thrusters at every 5.88 h ( $f_{\text{corr}} = 4.08 \text{ d}^{-1}$ ). The spacecraft stores the pixels of pre-selected targets only, similarly to the primary mission, but larger target pixel masks are allocated for less targets in the K2 fields to accommodate the larger pointing jitter and less frequent data download periods.

<sup>6</sup> <https://archive.stsci.edu/k2/>

Hence, the data acquisition principles are exactly similar to the stellar targets, only the combination of the small pixel masks of 2007 JJ<sub>43</sub> required additional steps during analysis.

The attitude of the spacecraft was adjusted by a few pixels shortly after the start of both campaigns. This did not affect the data of 2002 GV<sub>31</sub> but in the first 49 frames of Campaign 2, 2007 JJ<sub>43</sub> was too close to the edge of the mask and those were discarded. Apart from these adjustments, the largest correction movements were always smaller than a pixel and the root mean square of image shift offsets were 0.3 pixels for both campaigns. A closer inspection of the field-of-view movements revealed that the direction of motion reversed at the middle of the campaign and in some cases the correction maneuver did not occur and the telescope drifted for 11.76 h (instead of 5.88 h).

## 3. DATA REDUCTION

While in the case of 2002 GV<sub>31</sub>, the target pixel file contained a single stamp of  $23 \times 22$  pixels, the data extraction was much complex in the case of 2007 JJ<sub>43</sub>. Here, the total mask related to this object has been split to individual target stamps containing only  $1 \times 11$  or  $1 \times 13$  pixels. Hence, the first step of the reduction was the reconstruction of the effective section of the target CCD areas and the marking of the outlier pixels (in order to exclude them from the further data processing). In the case of 2002 GV<sub>31</sub>, we employed the PyKE package (Still & Barclay 2012) to create individual FITS frames for each timestamp while the combined

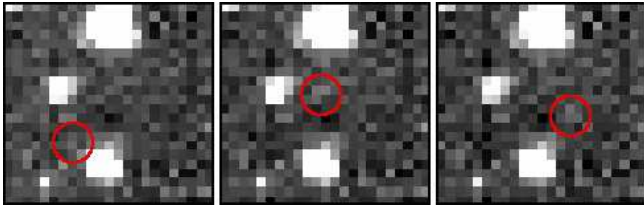


FIG. 2.— Detection of the motion of the faint TNO, 2002 GV<sub>31</sub> around its stationary point, on 1-day co-added images. These stamps are centered at  $\alpha = 11^{\text{h}}28^{\text{m}}38.8^{\text{s}}$ ,  $\delta = +05^{\circ}34'02''$  and cover the  $23 \times 22$  *Kepler* pixels, yielding a field-of-view of nearly  $1.5' \times 1.5'$ . The image orientation is related to *Kepler* sensors during these observations, i.e. north is roughly to the left while east is downwards.

and marked frame series for 2007 JJ<sub>43</sub> was created using the utilities of the FITSH<sup>7</sup> package (Pál 2012). Prior to the light curve analysis (see Sec. 4), for the subsequent data processing steps we employed various tasks of the FITSH package (esp. `fiign`, `fitrans`, `grtrans`, `grmatch`, `fiphot`, `fistar`).

Since the target pixel time series do not contain information regarding to the time variation of the astrometric solutions of the individual smaller stamps, frame registration had to be based on purely imaging data. Due to the fairly strange shape of the field containing the apparent path of 2007 JJ<sub>43</sub> (see. Fig. 1), automatic source identification and cross-matching algorithms based on triangulation matching (see also Pál & Bakos 2006) were not found to be effective<sup>8</sup>. Therefore, we manually selected seven prominent<sup>9</sup> stars distributed nearly uniformly in the field. Namely, we picked four stars located in the northern stripe and three stars in the southern stripe. Initial pixel coordinates for these stars have been acquired using the `imexam` tool of IRAF<sup>10</sup> on adjacent frame pairs belonging to events where the pointing of *Kepler* was changed abruptly. We found that this kind of manual analysis of 39 images were sufficient in order to bootstrap the astrometry and for the cross-identification procedure for all of the 3789 individual images.

After the cross-identification and the derivation of the differential transformations were performed, we used these transformations to register the images to the same system. Then, we stacked every tenth of the images after correcting of the background variations in order to obtain a master frame. This master image was created using a median averaging to exclude the effects of the cosmic hits, as well as to safely rule out the contribution of other moving objects<sup>11</sup>.

Photometry of 2007 JJ<sub>43</sub> was then performed using differential images (difference between the individual images and the aforementioned master image) where the aperture centroid coordinates were based on *Kepler*-centric apparent positions retrieved from the

<sup>7</sup> <http://fitsh.szofi.net/>

<sup>8</sup> The triangle parameter space is highly biased in this case while triangulation matching algorithms works most efficiently when the triangles have a nearly uniform distribution in this space.

<sup>9</sup> Bright, isolated stars which are close to the center of the stripes.

<sup>10</sup> IRAF is distributed by the National Optical Astronomy Observatory, which is operated by the Association of Universities for Research in Astronomy (AURA) under a cooperative agreement with the National Science Foundation.

<sup>11</sup> See <http://szofi.net/apal/astro/k2/tno/> for animations.

TABLE 1  
PHOTOMETRIC DATA OF 2007 JJ<sub>43</sub> AND 2002 GV<sub>31</sub>

Object	Time (JD)	Magnitude <sup>a</sup>	Error
2007 JJ <sub>43</sub>	2456893.044947	20.288	0.078
–	2456893.208405	20.686	0.111
–	2456893.228837	20.722	0.105
2002 GV <sub>31</sub>	2456839.65	23.680	0.606
–	2456839.75	22.862	0.402
–	2456839.85	22.957	0.403

NOTE. — Table 1 is published in its entirety in the electronic edition of the *Astrophysical Journal Letters*. A portion is shown here for guidance regarding its form and content.

<sup>a</sup> Magnitudes shown here are transformed to USNO-B1.0 *R* system, see text for further details.

NASA/Horizons service<sup>12</sup>. The instrumental aperture was chosen to be relatively small due to the faintness of the object. Despite the usage of differential images, the residual structures were significant due to the undersampled property of the *Kepler* camera. Namely, the spline-based interpolation throughout the registration process always introduces undershootings in case of stellar profiles with small FWHMs yielding characteristic features on the residual images (see e.g. Fig. 4 in Pál 2009). Photometric uncertainties have been estimated considering photon noise and measured background scatter in the aperture annuli. For the photon noise estimation, we used the gain values reported in the original FITS header, namely  $113.3 \text{ e}^-/\text{ADU}$ . As we will discuss later on (Sec. 4), this estimation was found to be reliable.

In the case of 2002 GV<sub>31</sub>, we followed a similar data flow for image reduction, with the exception that the frame registration was much easier due to the smaller size and the fewer number of stars (Fig. 2). Namely, the number of unambiguously identified background stars was three and the mean of the centroid shifts (in both directions) was used to obtain the offset values for the image registration. In addition, we binned the images into intervals of 0.1d in order to increase the signal in the frames. Hence, each frame on which photometry is performed were derived from  $\sim 5$  individual downlinked measurements. In all other aspects, the photometry was performed identically for the two objects.

For both objects, photometric magnitudes have been transformed into USNO-B1.0 *R* system (Monet et al. 2003). In the case of 2007 JJ<sub>43</sub>, we found that the unbiased residual of the photometric transformation between USNO and *Kepler* unfiltered magnitudes was 0.05 mag, while for 2002 GV<sub>31</sub> it was found to be 0.09 mag. Stars used for both objects have magnitudes spanning nearly homogeneously between  $R \approx 15$  and  $R \approx 19$ . Photometric data are displayed in Table 1.

#### 4. LIGHT CURVE ANALYSIS

The data produced from the baseline photometry consisted of time instance, magnitude and magnitude errors. 2224 data points belonged to 2007 JJ<sub>43</sub>, and 129 points to 2002 GV<sub>31</sub>, respectively. We tested that the photometric error estimates by the reduction pipeline are quite realistic. The mean determined photometric error of the entire dataset is 0.163 magnitudes, while the mean of the

<sup>12</sup> <http://ssd.jpl.nasa.gov/horizons.cgi>

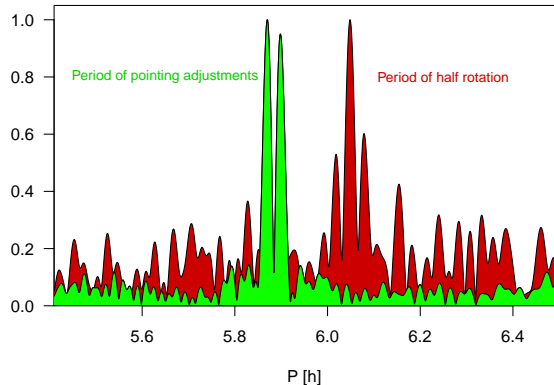


FIG. 3.— Fourier transform of the K2 light variation of the (278361)2007 JJ<sub>43</sub> normalized to 1 (red). The frequency axis was transformed to the time (period) dimension. In order to demonstrate that thanks to the motion of the TNO, the pointing adjustments were averaged out from the light variation, we plot the Fourier transform of the  $x$  coordinate of the centroid. The variations from the TNO rotation and the spacecraft pointing adjustment are clearly separated.

standard deviation of data points in the boxcar is 0.127 magnitudes. These values are comparable to each other within 30% accuracy. For later processing, the weights of the photometric data were set to be proportional to  $1/\sigma_i^2$ , where  $\sigma_i$  is the formal photometric error of each data points.

We also observed that this approach overweights the outliers on the bright side, and may introduce a distortion in the shape of the light curve. This is because error sources, such as residuals after image subtraction, scatter toward both directions (too faint and too bright), but the mean brightness is biased here, because the formal errors of bright-looking objects are much smaller, and they are given larger weights. Therefore at the bright wing of data distribution, the weights were downscaled by a function of the shape

$$\arctan \left[ 8 e^{-d^2/\mu^2} \right] + 0.3 \quad (1)$$

where  $d = m - m_0$ , the deviation of the measured  $m$  magnitudes from the mean value. We selected  $\mu \approx 4$  times the peak of the Fourier spectrum at the rotational period (0.15 for 2007 JJ<sub>43</sub> and 0.5 for 2002 GV<sub>31</sub>, respectively). Here the peak of the Gaussian curve is damped by the  $\arctan(\cdot)$  function acting on it, leading to a flat plateau around the center of the shape. We are convinced that this rescaling leads to more realistic weights than the crude estimates making use of the measured flux values. However, in order to avoid biasing the results in any way, we compared the results with and without weighting, and we experienced that they were practically identical – so the modified weights supported merely the better visualization.

The rotation periods were found by a Fourier analysis. The Fourier transform of the light curves were calculated by the `Period04` code (Lenz & Breger 2005). To exclude the light variation introduced by periodic systematics, we also calculated the periodograms of the pointing position of the telescope, the actual and the measured subpixel positions of the TNOs in each frames. We did not find periodic signals resulting from the sampling effects (there-

fore subpixel positions), but we identified the peak due to the pointing corrections with 4.05 cycle/d frequency (Fig. 3). This is close to the frequency peak belonging to a half rotation of 2007 JJ<sub>43</sub>, but they are still well separated, proving that the periodograms of the TNOs reflect the rotation.

## 5. RESULTS

### 5.1. (278361)2007 JJ<sub>43</sub>

(278361)2007 JJ<sub>43</sub> is an outer Kuiper belt object, likely in 2 : 1 resonance with Neptune (MPC 60235 2007). Based on its absolute magnitude at discovery ( $H_V = 3.9$ ) and the cluster average geometric albedo of  $p_V = 0.13^{+0.09}_{-0.07}$  for objects in the outer Kuiper belt (Lacerda et al. 2014), its likely effective diameter is  $D_{\text{eff}} = 610^{+170}_{-140}$  km. 2007 JJ<sub>43</sub> was also detected by the Southern Sky and Galactic Plane Survey for Bright Kuiper Belt Objects (Sheppard et al. 2011), and an R-band absolute magnitude of  $H_R = 3.2$  was associated to the object.

Benecchi & Sheppard (2013) detected a light curve of 2007 JJ<sub>43</sub>, with a peak-to-peak amplitude of  $0.13 \pm 0.02$  in the Sloan  $r'$  band. The most likely light curve (rotation) period they found was 6.04 h, or similarly likely its double period, 12.09 h. However, other periods (4.83/9.66 h) were also possible. The light curve was clearly non-sinusoidal. The absolute magnitude in this band was found to be  $H_{r'} = 4.17 \pm 0.20$ .

The period analysis confirmed the most likely solution of Benecchi & Sheppard (2013), namely  $6.048 \pm 0.018$  h. This is clearly the half of the rotation period, confirmed by the asymmetry of the phased light curve with  $P = 12.097 \pm 0.036$  h period (left panel of Fig. 4). Weighted means of the magnitude and corresponding phases were calculated in a boxcar of 68 data points. The standard deviation and the number of points in each bins resulted in an expected standard deviation (error bars) of  $\approx 0.015$  magnitudes for the binned points. The smoothed light curve shows two humps with equivalent minima and slightly different peaks. The full amplitude is  $0.100 \pm 0.005$  magnitude, the difference between the minima is 0.02 magnitudes. The asymmetry and the non-sinusoidal shape of the light curve reflects the uneven surface structures. These features are quite common for Solar System objects, e.g. a very similar light curve shape is observed for the main belt asteroid (52) Europa at certain observing circumstances (e.g. Michałowski et al. 2004). We can also conclude that the presented K2 measurement and the previous photometry of 2007 JJ<sub>43</sub> in Benecchi & Sheppard (2013) shows similar characteristics since in the case of TNOs, the phase and aspect angles varies rather slowly on the timescale of these observations.

### 5.2. 2002 GV<sub>31</sub>

2002 GV<sub>31</sub> is a dynamically cold classical Kuiper belt object. A recent evaluation of Johnson R-band MPC data and a conversion using  $V - R = 0.59 \pm 0.15$  (average for classicals) resulted in a V-band absolute magnitude of  $H_V = 6.1 \pm 0.6$ . 2002 GV<sub>31</sub> was observed, but not detected in any bands of the PACS camera on board the Herschel Space Observatory, in the framework of the "TNOs are Cool!" Open Time Key Pro-

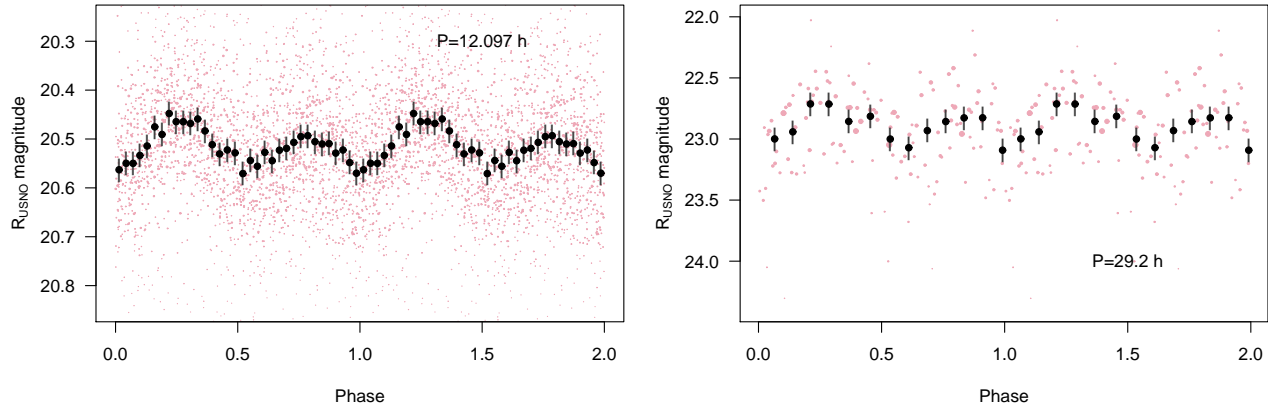


FIG. 4.— Left: phased light curve of (278361) 2007 JJ<sub>43</sub> (red points). The bold symbols with the error bars are binned values. Right: K2 light curve of 2002 GV<sub>31</sub>.

gram (Müller et al. 2009). Using the upper limits set by the non-detections, a modelling of the thermal emission of the target resulted in an upper limit of its size ( $D \lesssim 180$  km), and a lower limit on its geometric albedo ( $0.19 \lesssim p_V$ , see Vilenius et al. 2012, 2014). No light curve information is available for this target.

The first light curve of this object is shown in the right panel of Fig. 4, phased with the most likely rotation period of  $29.2 \pm 1.1$  h and showing a double peak. Since we had 129 photometric points from K2 in this case, they were binned into 13 points during one rotation, and the error bar of the binned points resulted to be 0.06 magnitudes. The full amplitude of the light variation is 0.35 magnitudes, which can be a sign of a more exposed asphericity than for 2007 JJ<sub>43</sub>. The most interesting feature of this TNO is its long rotation period, as most TNOs and Centaurs have rotation periods shorter than a day (Duffard et al. 2009; Benecchi & Sheppard 2013).

Longer periods are expected from synchronously locked, tidally evolved binary systems (see Pluto/Charon or Sila/Nunam, Grundy et al. 2012). It can explain the slow rotation of 2010 WG<sub>9</sub> (Rabinowitz et al. 2013) and can be plausible for 2002 GV<sub>31</sub> either. Moreover, observational statistics can explain binarity more likely for dynamically cold TNOs (Noll et al. 2008). In addition, statistics seem to prefer close orbits (Fig. 4 in Noll et al. 2008) which can also yield mutual events and hence strong light curve variations.

## 6. CONCLUSIONS

We clearly detected the rotational signal of two TNOs with *Kepler* during the K2 extended ecliptic survey mission. Since these objects are moving through the field-of-view, photometric data reduction requires special care in order to retrieve accurate flux information. Although the image processing needs complex steps, our results clearly show that the moving nature of these targets are also advantageous. Namely, differential photometric techniques strenuously reduce the effects of background sources, even in the crowdedness of *Kepler* fields and in the case of lower imaging resolution and undersampled stellar profiles. In addition, the employment of moving apertures removes the frequency aliases caused by the

pointing corrections of the spacecraft in every  $\sim 6$  hours.

All in all, we successfully demonstrated that it is feasible to observe faint TNOs around their stationary points with *Kepler*/K2 and this mission provides a unique way to monitor them continuously for many weeks. The scientific benefit of observing TNOs is the opportunity to provide an unbiased sample of rotational light curves – and hence data about shape, albedo and surface characteristics. This kind of information aids us to understand the nature and evolution of the outer Solar System.

Future space missions, like TESS and PLATO are not well suited to this kind of observations, therefore we encourage to include the brightest TNOs in each observing campaign to exploit this unique capability of the K2 Mission.

We thank the hospitality of the Veszprém Regional Centre of the Hungarian Academy of Sciences (MTA VEAB) where most of our work was carried out. We also thank the comments of the anonymous referee. This project has been supported by the Lendület-2009 and LP2012-31 Young Researchers Program, the Hungarian OTKA grants K-83790, K-109276 and K-104607 and by City of Szombathely under agreement no. S-11-1027. The research leading to these results has received funding from the European Community’s Seventh Framework Programme (FP7/2007-2013) under grant agreements no. 269194 (IRSES/ASK), no. 312844 (SPACEINN), and the ESA PECS Contract Nos. 4000110889/14/NL/NDe and 4000109997/13/NL/KML. Gy. M. Sz. and Cs. K. was supported by the János Bolyai Research Scholarship. Funding for the K2 spacecraft is provided by the NASA Science Mission directorate. The authors acknowledge the Kepler team for the extra efforts to allocate special pixel masks to track moving targets. All of the data presented in this paper were obtained from the Mikulski Archive for Space Telescopes (MAST). STScI is operated by the Association of Universities for Research in Astronomy, Inc., under NASA contract NAS5-26555. Support for MAST for non-HST data is provided by the NASA Office of Space Science via grant NNX13AC07G and by other grants and contracts.

## REFERENCES

- Benecchi, S. D., Sheppard, S. S. 2013, *AJ*, 145, 124
- Borucki, W. J., Koch, D., Basri, G., et al. 2010, *Science*, 327, 977

- Duffard, R.; Ortiz, J. L.; Thirouin, A.; Santos-Sanz, P.; Morales, N. 2009, *A&A*, 505, 1283
- Grundy, W. M., Benecchi, S. D., Rabinowitz, D. L. et al. 2012, *Icarus*, 220, 74
- Howell, S. B., Sobeck, C., Haas, M., et al. 2014, *PASP*, 126, 398
- Lacerda, P. 2005, PhD thesis, Leiden University
- Lacerda, P., Fornasier, S., Lellouch, E., et al. 2014, *ApJL*, 793, 2
- Minor Planet Circulars 60235, 2007
- Noll, K. S., Grundy, W. M., Chiang, E. I., Margot, J.-L. & Kern, S. D. In *The Solar System Beyond Neptune*, Eds. A. Barucci, H. Boehnhardt, D. Cruikshank, and A. Morbidelli. Univ. of Arizona Press, Tucson, pp. 345-363.
- Lenz P., Breger M., 2005, *CoAst*, 146, 53
- Michalowski, T.; Kwiatkowski, T.; Kaasalainen, M. et al. 2004, *A&A*, 416, 353
- Monet, D. G., Levine, S. E.; Canzian, B., et al. 2003, *AJ*, 125, 984
- Müller, T. G., Lellouch, E, Bönhardt, H. et al. 2009, *EM&P*, 105, 209
- Pál, A. 2009, PhD thesis, Eötvös Loránd University, Budapest, Hungary (arXiv:0906.3486)
- Pál, A. 2012, *MNRAS*, 421, 1825
- Pál, A., Bakos, G. Á., 2006, *PASP*, 118, 1474
- Rabinowitz, D., Schwamb, M. E., Hadjiyska, E., Tourtellotte, S. & Rojo, P. 2013, *AJ*, 146, 17
- Sheppard, S. S., Udalski, A., Trujillo, C., et al. 2011, *AJ*, 142, 98
- Still, M., Barclay, T.: *Astrophysics Source Code Library*, record ascl:1208.004, 2012
- Szabó, R., Sárneczky, K., Szabó, Gy. M., et al. 2015, *AJ*, 149, 112
- Vilenius, E., Kiss, C., Mommert, M. et al. 2012, *A&A*, 541, 94
- Vilenius, E., Kiss, C., Müller, T. et al. 2014, *A&A*, 564, 35